On the non-ergodicity of the Swendsen–Wang-Kotecký algorithm on the kagomé lattice

Bojan Mohar[1]‡ **and Jesús Salas**[2]

[1] Department of Mathematics, Simon Fraser University, Burnaby, B.C. V5A 1S6, Canada.

E-mail: `mohar@sfu.ca`

[2] Instituto Gregorio Millán and Grupo de Modelización, Simulación Numérica y Matemática Industrial, Universidad Carlos III de Madrid, Avda. de la Universidad, 30, 28911 Leganés, Spain.

E-mail: `jsalas@math.uc3m.es`

Abstract. We study the properties of the Wang–Swendsen–Kotecký cluster Monte Carlo algorithm for simulating the 3-state kagomé-lattice Potts antiferromagnet at zero temperature. We prove that this algorithm is not ergodic for symmetric subsets of the kagomé lattice with fully periodic boundary conditions: given an initial configuration, not all configurations are accessible via Monte Carlo steps. The same conclusion holds for single-site dynamics.

PACS numbers: 02.10.Ox 02.40.Re 02.50.Ga 05.50.+q 64.50.De

‡ On leave from Department of Mathematics, IMFM & FMF, University of Ljubljana, Ljubljana, Slovenia.

1. Introduction

The q-state Potts model [1, 2, 3] is certainly one of the simplest and most studied models in Statistical Mechanics. However, despite many efforts over more than 50 years, its *exact* solution (even in two dimensions) is still unknown. The ferromagnetic regime is the best understood case: there are exact (albeit not always rigorously proved) results for the location of the critical temperature, the order of the transition, etc. The antiferromagnetic regime is less understood, partly because universality is not expected to hold in general (in contrast with the ferromagnetic regime case); in particular, critical behaviour may depend on the lattice structure of the model. One interesting feature of this antiferromagnetic regime is that it exhibits non-zero ground-state entropy (without frustration) for large enough values of q on a given lattice. This provides an exception to the third law of thermodynamics [5, 6]. In addition, a zero-temperature phase transition may occur for certain values of q and certain lattices: e.g., the models with $q = 2, 4$ on the triangular lattice, and $q = 3$ on the square and kagomé lattices, cf. [4] and references therein.

In addition to its intrinsic theoretical interest, the antiferromagnetic 3–state Potts model on the kagomé lattice also plays an important role in condensed–matter physics. Several experimental systems are proposed to be modelled by antiferromagnetic n-component $O(n)$ spin models on the kagomé lattice [7, 8, 9, 10, and references therein]. For both the XY ($n = 2$) and Heisenberg ($n = 3$) models, there are theoretical arguments showing that, in the zero-temperature limit, their ground states can be described by the 3–state antiferromagnetic Potts model. Furthermore, Huse and Rutenberg [8] showed that exactly at zero temperature, the later model has a SOS (or height) representation, and it is critical.

The standard q-state Potts model can be defined on any finite undirected graph $G = (V, E)$ with vertex set V and edge set E. On each vertex $i \in V$ of the graph G, we place a spin $\sigma(i) \in \{1, 2, \ldots, q\}$, where $q \geq 2$ in an integer. The spins interact via a Hamiltonian

$$H(\{\sigma\}) = -J \sum_{e=ij\in E} \delta_{\sigma(i),\sigma(j)}, \tag{1}$$

where the sum is over all edges $e \in E$, $J \in \mathbb{R}$ is the coupling constant, and $\delta_{a,b}$ is the Kronecker delta. The *Boltzmann weight* of a configuration is then $e^{-\beta H}$, where $\beta \geq 0$ is the inverse temperature. The *partition function* is the sum, taken over all configurations, of their Boltzmann weights:

$$Z_G^{\text{Potts}}(q, \beta J) = \sum_{\sigma:\, V \to \{1,2,\ldots,q\}} e^{-\beta H(\{\sigma\})}. \tag{2}$$

A coupling J is called *ferromagnetic* if $J \geq 0$, as it is then favored for adjacent spins to take the same value; and *antiferromagnetic* if $-\infty \leq J \leq 0$, as it is then favored for adjacent spins to take different values. The zero-temperature ($\beta \to +\infty$) limit of the antiferromagnetic ($J < 0$) Potts model has an interpretation as a colouring problem: the limit $\lim_{\beta\to+\infty} Z_G^{\text{Potts}}(q, -\beta|J|) = P_G(q)$ is the *chromatic polynomial*, which

gives the number of proper q-colourings of G. A *proper q-colouring* of G is a map $\sigma\colon V \to \{1, 2, \ldots, q\}$ such that $\sigma(i) \neq \sigma(j)$ for all pairs of adjacent vertices $ij \in E$. In other words, a proper q-colouring of a graph G is a colouring of the vertices of G such that any pair of nearest-neighbour vertices are not coloured alike.

For many Statistical Mechanics systems for which an exact solution is not known, (Markov chain) Monte Carlo simulations [11, 12] have become a very valuable tool to extract physical information. One popular Monte Carlo algorithm for the *antiferromagnetic q-state* Potts model is the Wang–Swendsen–Kotecký (WSK) *non-local* cluster dynamics [13, 14]. Even though at any positive temperature the WSK algorithm satisfies *all* the necessary conditions in order to work, *exactly* at zero temperature, one condition (i.e., ergodicity) may not hold, and therefore, the algorithm can no longer be used! A Monte Carlo algorithm is *ergodic* (or irreducible) if it can eventually get from each state (or configuration) to every other state. While this condition is easy to check for the WSK algorithm at any positive temperature, it becomes a highly non-trivial question at zero temperature for non-bipartite graphs.

It is interesting to note that at zero temperature, the basic moves of the WSK dynamics correspond to the so-called *Kempe changes*, introduced by Kempe in his unsuccessful proof of the four-colour theorem [15, Section 7.3.1] (see also [16] anc check [17] for additional references). This zero-temperature algorithm (disguised under the name of 'path–flipping' algorithm) has already been used by several authors [8, 9]. In particular, Huse and Rutenberg [8] noted (see their footnote 13) that for fully periodic boundary conditions this algorithm is not ergodic; but we are not aware of any (rigorous) proof of this claim in the literature.

It is also worth noticing that for q-state Potts antiferromagnets without frustration (e.g., $q \geq 3$ for the kagomé lattice), single–spin flips are a (proper) subset of the set of Kempe moves. Therefore, the non-ergodicity of the later dynamics implies the non-ergodicity of single–flip algorithms (which include the well–known Metropolis algorithm [12]). For positive temperature, the WSK algorithm (on any graph) always include single-site moves as a special case.

Although the Potts model can be defined on any graph G, in Statistical Mechanics one is mainly interested in 'large' regular graphs with fully periodic boundary conditions (i.e., embedded on a torus). Boundary conditions of this type are usually chosen to minimize finite-size-scaling effects [18]. Therefore, we will focus on the commonest set-up in actual Monte Carlo simulations: finite symmetric subsets of the kagomé lattice wrapped on a torus.

The ergodicity of the WSK algorithm for the zero-temperature q-state Potts antiferromagnet on the kagomé lattice embedded on a torus is only an open question for $q = 3, 4$. For $q = 2$ (the Ising model) it is trivially non-ergodic, as each WSK move is equivalent to a global spin flip. It is interesting to remark that there is an analytic solution for the Ising model on the kagomé lattice [19]; this solution shows that there is no phase transition in the whole antiferromagnetic regime, including zero temperature, where the system displays frustration. On the contrary, for $q \geq 5$ the

algorithm is ergodic (see Section 2 for more details). Among the two unknown cases, $q = 3$ is the most interesting one, because the system is expected to be critical at zero temperature [8].

The main result of this paper is to provide a *proof* of the non-ergodicity of the zero–temperature WSK algorithm for the 3–state Potts antiferromagnet on symmetric subsets of the kagomé lattice with fully periodic boundary conditions. We find that the ground-state configuration space (i.e., the set of all proper 3-colourings of the given kagomé graph) can be split into *at least* two 'ergodicity classes' (or Kempe equivalence classes), such that one class is unreachable using Kempe moves from the other one, and vice versa. This also means that single–flip dynamics is also non-ergodic for such systems. In this case, each ground-state configuration constitutes an ergodicity class. Therefore, these zero-temperature Monte Carlo algorithms simply do not work, and new algorithms satisfying all the required properties should be sought in order to simulate such systems. Furthermore, no reasonable algorithm is known at present to our knowledge, which is ergodic at zero temperature. It is an interesting open problem to find one.

Our basic strategy in this paper goes as follows: We start with the observation that the kagomé lattice is the medial of the triangular lattice. § In particular, for the reasons explained above, we are interested in the kagomé graphs $T'(3L, 3L)$ which are the medials of the regular triangulations $T(3L, 3L)$ of the torus (roughly speaking, these triangulations are subsets of the triangular lattice of linear size $(3L) \times (3L)$ with fully periodic boundary conditions). We then show that any proper 3–colouring ϕ of the kagomé lattice $T'(3L, 3L)$ can be viewed as a particular proper 4–colouring f of the 'doubled' triangulation $T(6L, 6L)$, and that any WSK transition made on ϕ corresponds to a sequence of WSK moves performed on f in $T(6L, 6L)$. We call the colourings f of $T(6L, 6L)$ that are obtained from 3–colourings of the kagomé lattice *special colourings* of $T(6L, 6L)$. This correspondence enables us to use the results of Ref. [20] about the non-ergodicity of the zero-temperature WSK algorithm for the 4–state Potts antiferromagnet on the triangulations $T(3L, 3L)$ with $L \geq 2$.

Proper 4–colourings of a triangulation embedded on a torus are rather special, as they can be regarded as maps from a sphere to the torus (using the tetrahedral representation of the spin). This basic observation allowed us to borrow concepts from algebraic topology; in particular, the degree $\deg(f)$ of a proper 4–colouring f. This approach was pioneered by Fisk [21, 22, 23], who also showed that $\deg(f)$ on any 3–colourable triangulation of the torus is always a multiple of 6 (the triangulations $T(3L, 3L)$ are indeed 3–colourable). We then showed that $\deg(f) \pmod{12}$ is an invariant under a Kempe move. Therefore, if we are able to find two 4–colourings f and g with degrees $\deg(f) \pmod{12} = 0$ and $\deg(g) \pmod{12} = 6$, then there are *al least* two Kempe equivalence classes, and therefore the zero–temperature WSK algorithm is not ergodic. For all triangulations $T(3L, 3L)$ with $L \geq 2$ we were able to find such two 4–colourings [20].

---

§ See Section 3 for a precise definition of the medial graph $M(G)$ of a graph G.

In this paper, we apply these results to the subset of special 4–colourings of $T(6L, 6L)$: for any $L \geq 1$, we find that there are two special 4–colourings f and g with degrees congruent with 0 and 6 modulo 12, respectively. Therefore, we cannot get f from g (or vice versa) using Kempe moves, even in the larger configuration space of all proper 4–colourings of $T(6L, 6L)$. The same is true if we restrict ourselves to the smaller set of *special* proper 4–colourings of $T(6L, 6L)$, which corresponds to the set of proper 3–colourings of $T'(3L, 3L)$. Therefore, the non-ergodicity of the Kempe dynamics for these kagomé graphs follows.

As explained above, our approach, based on algebraic topology, can only be applied to proper 4–colourings of the triangulations $T(3L, 3L)$, or to proper 3–colourings of the kagomé graphs $T'(3L, 3L)$ (by exploiting that T' is the medial of T). Unfortunately, it cannot be extended to study the ergodicity of the WSK algorithm for the 4–state kagomé–lattice antiferromagnet. It is curious that our methods work for the two models that have a height representation and are critical at zero temperature [8]. It would be interesting to translate our findings into the height language [10]. This may lead to a improved (and hopefully) ergodic algorithm.

Finally, one might consider simulating the 3–state Potts antiferromagnet using the WSK algorithm at a small but *positive* temperature. In this case, the algorithm is indeed ergodic and satisfies all the required properties to work fine. However, the only way we can reach from one ergodicity class to another is through a non-zero-energy configuration (or non–proper 3–colouring). But these configurations are exponentially suppressed in this limit: we have to pay a penalty of $e^{-\beta|J|}$ for each pair of neighbouring vertices coloured alike. Therefore, it is unlikely for small enough temperatures that the system visit more than one class. Furthermore, it would be very interesting to consider, in addition to the standard observables, new observables specifically designed to 'feel' the nonergodicity of the algorithm, and to study numerically how their autocorrelation times behave as we approach to zero temperature.

The paper is organized as follows: In Section 2 we introduce our basic definitions, and review what is known in the literature about the problem of the ergodicity of the Kempe dynamics. In Section 3 we consider edge-colourings and relate them first to three-colourings of the kagomé graph and then to special colourings of triangulations $T(6L, 6M)$. In Section 4 we prove our main result about the non-ergodicity for symmetric kagomé graphs $T'(3L, 3L)$.

2. Basic Setup

Let $G = (V, E)$ be a finite undirected graph with vertex set V and edge set E. Then for each graph G there exists a polynomial P_G with integer coefficients such that, for each $q \in \mathbb{Z}_+$, the number of proper q-colourings of G is precisely $P_G(q)$. This polynomial P_G is called the *chromatic polynomial* of G. The set of all proper q-colourings of G will be denoted as $\mathcal{C}_q = \mathcal{C}_q(G)$ (thus, $|\mathcal{C}_q(G)| = P_G(q)$).

It is far from obvious that $Z_G^{\text{Potts}}(q, \beta J)$ [cf. (2)], which is defined separately for

each positive integer q, is in fact the restriction to $q \in \mathbb{Z}_+$ of a *polynomial* in q. But this is in fact the case, and indeed we have:

Theorem 2.1 (Fortuin–Kasteleyn [24, 25] representation of the Potts model)
For every integer $q \geq 1$, we have

$$Z_G^{\text{Potts}}(q, v) \;=\; \sum_{A \subseteq E} q^{k(A)} \, v^{|A|} \,, \tag{3}$$

where $v = e^{\beta J} - 1$, and $k(A)$ denotes the number of connected components in the spanning subgraph (V, A).

The foregoing considerations motivate defining the *Tutte polynomial* of the graph G:

$$Z_G(q, v) \;=\; \sum_{A \subseteq E} q^{k(A)} \, v^{|A|} \,, \tag{4}$$

where q and v are commuting indeterminates. This polynomial is equivalent to the standard Tutte polynomial $T_G(x, y)$ after a simple change of variables. If we set $v = -1$, we obtain the *chromatic polynomial $P_G(q) = Z_G(q, -1)$*. In particular, q and v can be taken as complex variables. See Ref. [26] for a recent survey.

As explained in the Introduction, we will focus on kagomé lattices that are related to certain regular triangulations embedded on the torus. The class of regular triangulations of the torus with degree six is characterized by the following theorem:

Theorem 2.2 (Altschulter [27]) *Let T be a triangulation of the torus such that all vertices have degree six. Then T is one of triangulations $T(r, s, t)$, which are obtained from the $(r + 1) \times (s + 1)$ grid by adding diagonals in the squares of the grid as shown in Figure 1, and then identifying opposite sides to get a triangulation of the torus. In $T(r, s, t)$ the top and bottom rows have r edges, the left and right sides s edges. The left and right side are identified as usual; but the top and the bottom row are identified after (cyclically) shifting the top row by t edges to the right.*

In Figure 1 we have displayed the triangulation $T(6, 2, 2)$ of the torus. We will represent these triangulations as embedded on a rectangular grid with three kinds of edges: horizontal, vertical, and diagonal. The three-colourability of the triangulations $T(r, s, t)$ is given by the following result [20]:

Proposition 2.3 *The triangulation $T(r, s, t)$ is three-colourable if and only if $r \equiv 0$ (mod 3) and $s - t \equiv 0 \pmod{3}$.*

In Monte Carlo simulations, it is usual to consider toroidal boundary conditions with no shifting, so $t = 0$. Then, the three-colourability condition reduces to the standard result $r, s \equiv 0 \pmod{3}$. In general, we will consider the following triangulations of the torus $T(3L, 3M, 0) = T(3L, 3M)$ with $L, M \geq 1$. The unique three-colouring c_0 of $T(3L, 3M)$ can be described as:

$$c_0(x, y) \;=\; \mathrm{mod}(x + y - 2, 3) + 1 \,, \quad 1 \leq x \leq 3L \,, \quad 1 \leq y \leq 3M \,, \tag{5}$$
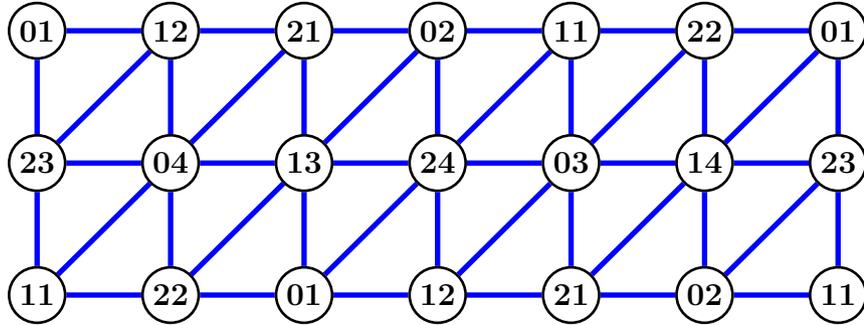
Figure 1. The triangulation $T(6,2,2) = \Delta^2 \times \partial\Delta^3$ of the torus. Each vertex x of $T(6,2,2)$ is labelled by two integers ij, where i (resp. j) corresponds to the associated vertex in Δ^2 (resp. $\partial\Delta^3$). The vertices of Δ^2 are labelled $\{0,1,2\}$, while the vertices of $\partial\Delta^3$ are labelled $\{1,2,3,4\}$. The triangulation $T(6,2,2)$ has 12 vertices, and those in the figure with the same label should be identified.

where we have explicitly used the above-described embedding of the triangulation $T(3L, 3M)$ in a square grid.

Finally, in most Monte Carlo simulations one usually considers tori of aspect ratio one: i.e., $T(3L, 3L)$. This is the class of triangulations we are most interested in from the point of view of Statistical Mechanics.

2.1. Kempe changes

Given a graph $G = (V, E)$ and $q \in \mathbb{N}$, we can define the following dynamics on $\mathcal{C}_q$: Choose uniformly at random two distinct colours $a, b \in \{1, 2, \ldots, q\}$, and let G_{ab} be the induced subgraph of G consisting of vertices $x \in V$ for which $\sigma(x) \in \{a, b\}$. Then, independently for each connected component of G_{ab}, with probability $1/2$ either interchange the colours a and b on it, or leave the component unchanged. This dynamics is the zero–temperature limit of the Wang–Swendsen–Kotecký (WSK) cluster dynamics [13, 14] for the antiferromagnetic q-state Potts model. This zero–temperature Markov chain leaves invariant the uniform measure over proper q-colourings; but its irreducibility cannot be taken for granted.

The basic moves of the WSK dynamics correspond to Kempe changes (or K-*changes*). In each K-change, we interchange the colours a, b on a given connected component (or K-*component*) of the induced subgraph G_{ab}.

Two q-colourings $c_1, c_2 \in \mathcal{C}_q(G)$ related by a series of K-changes are *Kempe equivalent* (or K$_q$-*equivalent*). This (equivalence) relation is denoted as $c_1 \overset{q}{\sim} c_2$. The equivalence classes $\mathcal{C}_q(G)/ \overset{q}{\sim}$ are called the *Kempe classes* (or K$_q$-*classes*). The number of K$_q$-classes of G is denoted by $\kappa(G, q)$. Then, if $\kappa(G, q) > 1$, the zero-temperature WSK dynamics is not ergodic on G for q colours.

In this paper, we will consider two q-colourings related by a *global* colour permutation to be the same. In other words, a q-colouring is actually an equivalence

class of standard q-colourings modulo global colour permutations. Thus, the number of (equivalence classes of) proper q-colourings is given by $P_G(q)/q!$. This convention will simplify the notation in the sequel.

2.2. The number of Kempe classes

In this section we will briefly review what it is known in the literature about the number of Kempe equivalence classes for several families of graphs. The first result implies that WSK dynamics is ergodic on any bipartite graph:‖

Proposition 2.4 (Burton & Henley [28], Ferreira & Sokal [29], Mohar [17])
Let G be a bipartite graph and $q \geq 2$ an integer. Then, $\kappa(G, q) = 1$.

It is worth noting that Lubin and Sokal [30] showed that the WSK dynamics with 3 colours is not ergodic on any square–lattice grid of size $3M \times 3N$ (with M, N relatively prime) wrapped on a torus. These graphs are indeed non-bipartite.

   The second type of results deals with graphs of bounded maximum degree Δ, and shows that $\kappa(G, q) = 1$ whenever q is large enough:

Proposition 2.5 (Jerrum [31] and Mohar [17]) *Let Δ be the maximum degree of a graph G and let $q \geq \Delta + 1$ be an integer. Then $\kappa(G, q) = 1$. If G is connected and contains a vertex of degree $< \Delta$, then also $\kappa(G, \Delta) = 1$.*

This result implies that for any kagomé lattice T' with $\Delta = 4$, $\kappa(T', q) = 1$ for any $q \geq \Delta + 1 = 5$. Notice that the cases $q = 2, 3, 4$ are not covered by the above proposition.

   Finally, if we consider planar graphs the situation is better understood. One of the authors proved that

Theorem 2.6 (Mohar [17], Theorem 4.4) *Let G be a three-colourable planar graph. Then $\kappa(G, 4) = 1$.*

Corollary 2.7 (Mohar [17], Corollary 4.5) *Let G be a planar graph and $q > \chi(G)$. Then $\kappa(G, q) = 1$.*

These results imply that WSK for $q \geq 4$ is ergodic on any three-colourable planar graph. But we cannot use these results, as none of our graphs is planar.

   The main theorem for triangulations appears in Ref. [23] and involves the notion of the degree of a four-colouring, whose definition is deferred to the next section.

Theorem 2.8 (Fisk [23]) *Suppose that T is a triangulation of the sphere, projective plane, or torus. If T has a three-colouring, then all four-colourings with degree divisible by 12 are Kempe equivalent.*

   In a previous paper [20], we proved a series of results that are of great importance in the present work. The first theorem ensures the existence of a Kempe invariant for the class of three-colourable triangulations of a closed orientable surface.

‖ All the cited authors have discovered this theorem independently.

Theorem 2.9 *Let T be a three-colourable triangulation of a closed orientable surface. If f and g are two four-colourings of T related by a Kempe change on a region R, then*

$$\deg(g) \ \equiv \ \deg(f) \pmod{12}. \tag{6}$$

Note that the class of three-colourable triangulations of a closed orientable surface contains and it is wider than the class $T(3L, 3M)$ we are interested in. This theorem and Fisk's theorem 2.8, imply the following Corollary:

Corollary 2.10 *Let T be a three-colourable triangulation of the torus. Then $\kappa(T, 4) > 1$ if and only if there exists a four-colouring f with $\deg(f) \equiv 6 \pmod{12}$.*

For symmetric triangulations $T(3L, 3L)$ we were able to prove the following result:

Theorem 2.11 *For any triangulation $T(3L, 3L)$ with $L \geq 2$ there exists a four-colouring f with $\deg(f) \equiv 6 \pmod{12}$. Hence, $\kappa(T(3L, 3L), 4) > 1$. In other words, the WSK dynamics for four-colourings on $T(3L, 3L)$ is non-ergodic.*

For non-symmetric triangulations $T(3L, 3M)$ our results can be summarized in the following theorem:

Theorem 2.12 *For any triangulation $T(3L, 3M)$ with any $L \geq 3$ and $M \geq L$, there exists a four-colouring f with $\deg(f) \equiv 6 \pmod{12}$. Consequently, the WSK dynamics for four-colourings of $T(3L, 3M)$ is non-ergodic.*

For triangulations $T(6, 3M)$ with $M \geq 2$, we could only prove the non-ergodicity of the WSK dynamics for $q = 4$ when $M = 2p$ with odd p, while this dynamics is ergodic at least for the triangulation $T(6, 9)$. Finally, we also proved that the WSK dynamics for $q = 4$ is always ergodic on any triangulation of the type $T(3, 3M)$ with $M \geq 1$.

3. Edge-colourings of triangulations of the torus

Four-colourings of triangulations of the 2-dimensional sphere are in a bijective correspondence with three other kinds of colourings: edge-colourings, Heawood colourings, and local colourings. When treated on the torus (or on any orientable surface of positive genus), these notions are no longer equivalent to each other, but there is a nice hierarchy among them as shown by Fisk [23]. Under this hierarchy, every 4-colouring induces an edge-colouring, every edge-colouring induces a Heawood colouring, every Heawood colouring induces a local colouring, and all these correspondences are 1-1. However, none of these implications can be reversed.

An *edge-colouring* P is a partition of the edges of a triangulation T intro three classes, so that each triangular face of T has one edge in each class. This is equivalent

---

P The usual definition of edge-colourings is by colouring the edges in such a way that edges incident to the same vertex receive distinct colours. In our definition, this actually works for the dual graph of the triangulation. Another interpretation is to view edge-colourings as vertex 3-colourings of the medial graph $M(G)$, which we shall do in the sequel.

to a proper three-colouring on the medial graph $T' = M(T)$ of the triangulation T. (The precise definition of the medial graph is given below.) In particular, if $T = T(3L, 3M)$, then $T' = T'(3L, 3M)$ is a *kagomé graph* embedded on a torus. On Figure 2 we show the particular case of $T'(4, 3)$.
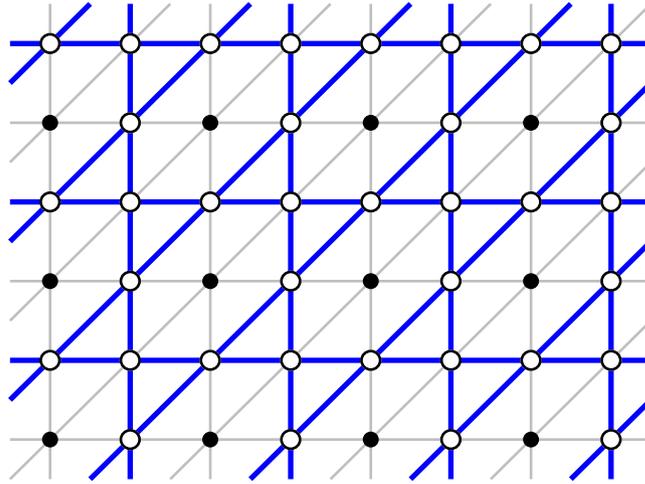
Figure 2. Kagomé lattice $T'(4, 3)$: the vertex set is given by the white circles ($\circ$) and the edge set is given by the thick lines. This graph is the medial graph of the triangulation $T(4, 3)$, with vertex set given by the solid black dots ($\bullet$) and edge set given by the thin gray lines.

As mentioned above, there is a hierarchy among these types of colourings, see [23, Proposition 25]. The simplest case of this hierarchy is the following one.

Proposition 3.1 *Let T be a triangulation of a surface. Every four-colouring of T induces an edge-colouring of T, and this correspondence is* 1-1.

Remarks. 1. The reverse implication is false. Most triangulations have edge-colourings that are not induced by any four-colouring. However, the two notions are equivalent for triangulations of the sphere.

2. It is usually assumed that the zero-temperature triangular-lattice 4–state Potts antiferromagnet is *equivalent* to the zero-temperature kagomé lattice 3-state Potts antiferromagnet. This is *not* true on any surface other than the sphere, as there might be edge-colourings not induced by four-colourings. See an example below.

Let us explain how to obtain the edge-colouring induced by a given four-colouring of a triangulation T. We will illustrate the general ideas with an example displayed in Figure 3: In (a) we plot a particular four-colouring f with $\deg(f) = 0$ of $T = T(3, 3)$. The edge-colouring g induced by f is depicted in Figure 3(b). It is obtained as follows: For each edge of T, we assign to the edge colour 1 if its end vertices are coloured 12 or 34; the edge will get colour 2 if its end vertices are coloured 13 or 24; and the edge gets colour 3 if its end vertices are coloured 14 or 23. The three vertices on any triangular
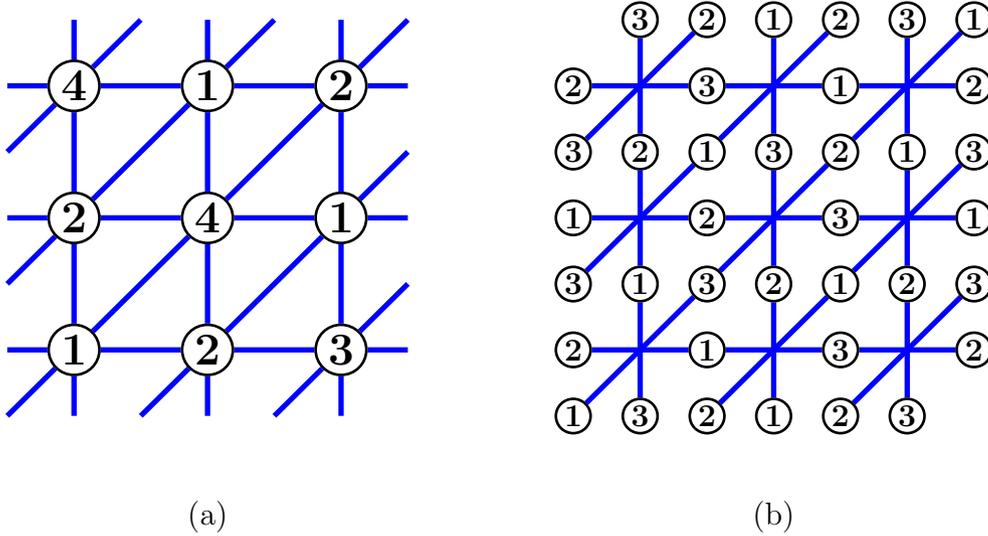
**Figure 3.** (a) A four-colouring f of $T(3,3)$ with $\deg(f) = 0$. (b) The edge-colouring induced by f.

face $t \in T$ are coloured differently by f, thus the stated procedure colours the edges of t with three distinct colours.

We define a *Kempe region* for an edge-colouring [23] in a similar fashion as for four-colourings. This is a region R of the triangulation T whose boundary has all edges of the same colour c. Then we can *exchange* the two colours different from c on all edges in R. Two edge-colourings are *K-equivalent* if one can be obtained from the other by a sequence of exchanges on Kempe regions.

Proposition 3.2 *If two four-colourings of a triangulation G are K-equivalent, then their induced edge-colourings are also K-equivalent.*

PROOF. Since the K-equivalence of four-colourings of G is generated by K-exchanges on the regions of the triangulation, it suffices to prove that a K-exchange for a four-colouring f made on a region R corresponds to the exchange performed on the same region for the induced edge-colouring ψ. Indeed, since R is a Kempe region for f, all edges on the boundary of R have their vertices coloured by the same pair of colours, say a, b. This implies that these edges have the same colour c under the edge-colouring ψ. Now, exchanging the two colours different from a, b on the vertices in the region R has the effect on the induced edge-colouring that is precisely the same as the exchange of edge-colours different from c on the edges in R. This completes the proof. ∎

It is natural to ask if a converse of Proposition 3.2 may hold. Unfortunately, the answer is negative. Even more, an edge-colouring ψ induced by a four-colouring f may be K-equivalent to an edge-colouring that is not induced by any four-colouring. Figure 4 shows an example of such a case.
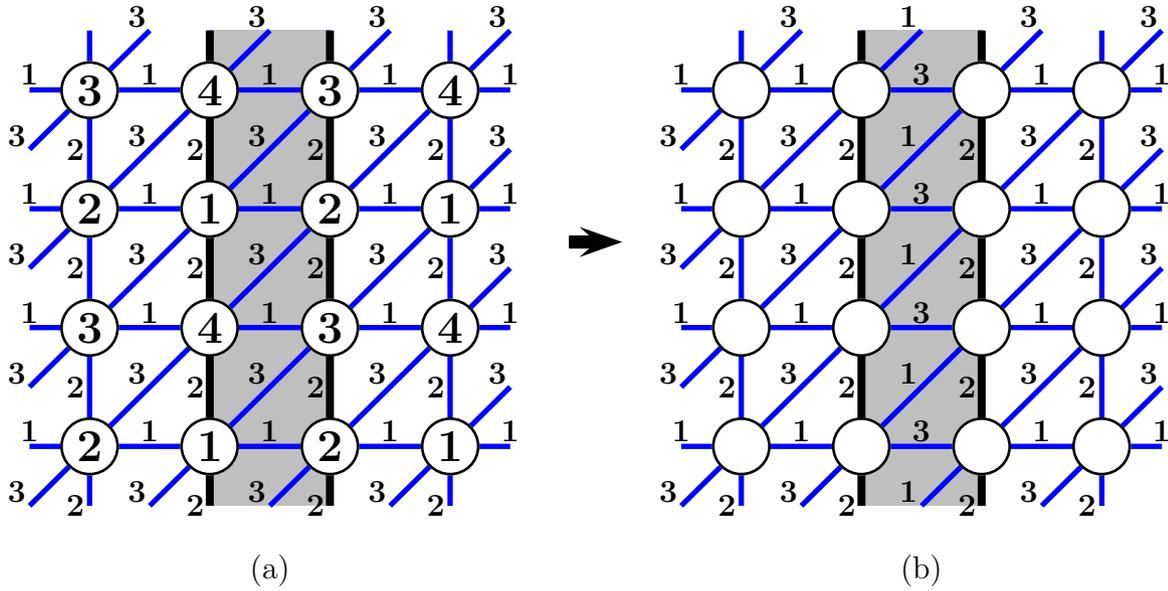
Figure 4. Example showing that the converse of Proposition 3.2 cannot be true. In panel (a) we show a 4-colouring of the triangulation $T(4,4)$ and its associated edge-colouring. The shaded triangles form a Kempe region for this edge-colouring. In panel (b), we display the new edge-colouring after the Kempe change. The exchange yields an edge-colouring that is not induced by any four-colouring. This example can be generalized to any triangulation $T(2n, 2m)$, with $n, m \geq 2$.

Although there are at least as many edge-colourings as there are four-colourings, the number of K-equivalence classes of four-colourings might be bigger or might be smaller than the number of equivalence classes of edge-colourings.

Our analysis can be simplified by introducing the *medial graph* $T' = M(T) = (V', E')$ of a triangulation T.

Let us first define the medial graph G' of a graph G (not necessarily a triangulation) embedded on a surface S. It is convenient to first define the *dual graph* $G^* = (V^*, E^*)$ of G, which is also embedded on S. This dual graph is built in the standard way as follows: To each face f in G, there corresponds a dual vertex $f^* \in V^*$; and for every edge $e \in E$, we draw a dual edge $e^* \in E^*$. If the original edge e lies on the intersection of two faces f and h (possibly $f = h$), then the corresponding dual edge e^* joins the dual vertices $f^*, h^* \in V^*$. We can draw G and G^* on S in such a way that each edge $e \in E$ intersects its corresponding dual edge $e^* \in E^*$ exactly once. (See Figure 5 for an example on the sphere.)

Then, the *medial graph* $G' = (V', E')$ of $G = (V, E)$ is constructed as follows: To each unique intersection between an edge $e \in E$ and its dual edge $e^* \in E^*$, there corresponds a vertex of the medial graph $v' \in V'$. (See Figure 5 where the vertices of the medial graph are depicted as open white circles.) It is clear that the medial graph G' is also embedded on S, and that G' is a regular graph of degree 4. Finally, the role played in this construction by G and its dual G^* is symmetric; therefore, the medial
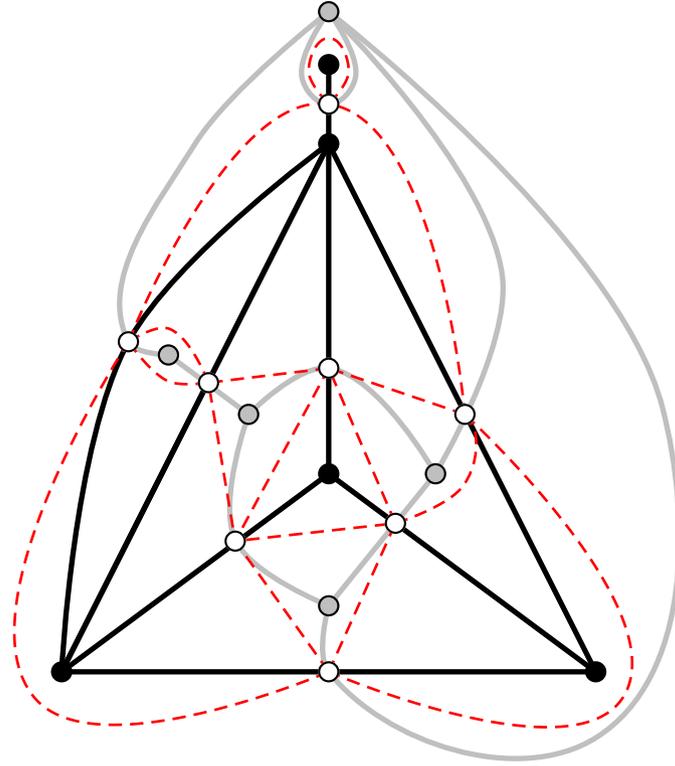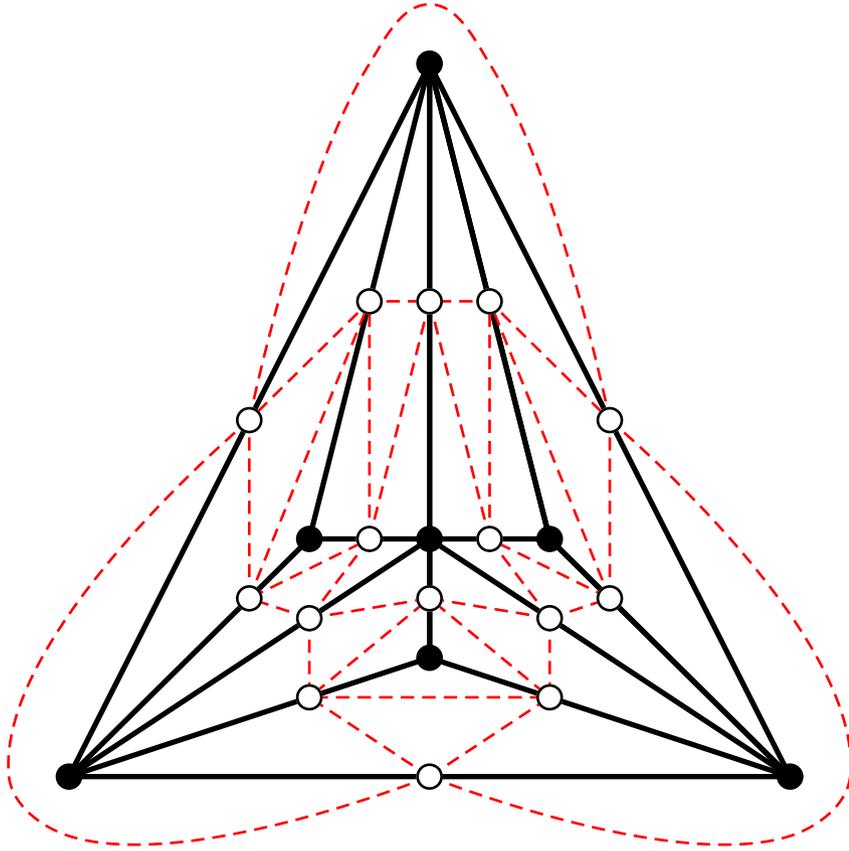
Figure 5. Graph $G = (V, E)$ embedded on the sphere. The vertices of V are depicted as solid black circles, and the edges of E as solid thick lines. The dual graph $G^* = (V^*, E^*)$ is represented as follows: the vertex set is depicted as solid gray circles, and the edge set as solid thick gray lines. Finally, the medial graph $G' = (V', E')$ is given by a vertex set drawn as open white circles, and by the edge set depicted as dashed thin (red) lines.

graph of G coincides with the medial of its dual $(G^*)' = G'$.

Edge-colourings of a triangulation $T = (V, E)$ embedded on a surface S can be regarded as three-colourings of the vertices of the corresponding medial graph $T' = M(T)$, which is also embedded on S. In T' there are two types of faces: triangular faces inside any triangular face of T, and faces with d_i sides containing every vertex $i \in V$ of degree d_i. (See Figure 6 for an example of a triangulation embedded on the sphere.) Notice that the medial graph T' of a triangulation T is not a triangulation of S (with the exception when $T = K_4$). A Kempe change on an edge-colouring of T has precisely the same effect as a standard Kempe change on T'.

The medial graph $T' = (V', E')$ can be regarded as a particular subgraph of another triangulation $T'' = (V'', E'')$ on the same surface that is obtained by adding back the original vertices of T, and also adding the edges joining each $v \in V$ with the vertices in V' corresponding to the edges of T incident with v. The vertices of T'' are simply $V'' = V \cup V'$. The edges of T'' are given by $E'' = E' \cup \widetilde{E}$. The second edge set $\widetilde{E}$ is constructed as follows: To each original edge $ab \in E$, the medial graph T' assigns a new vertex x. Then, the contribution of the edge $ab \in E$ to $\widetilde{E}$ consists of two edges ax

Figure 6. Triangulation $T = (V, E)$ of the sphere. The vertices of V are depicted as solid black circles, and the edges of E as solid thick lines. Its medial graph $T' = (V', E')$ is represented as follows: the vertices are depicted as open white circles, and the edges as dashed thin lines. The triangulation $T'' = (V'', E'')$ is constructed as follows: the vertices in V'' are those of V and V' (i.e., all circles, open or solid in the picture). The edges in E'' are all edges in the picture (dashed and solid); notice that each edge in E now corresponds to two edges in E''. For simplicity, we have not depicted T^*, the dual graph of T.

and xb. Notice that the degree in T'' of the vertices i in V (resp. V') is d_i (resp. six). The triangulation T'' can be constructed directly from T by inserting a new vertex in the middle of each edge of T and then inserting three edges joining the added vertices in each triangular face. Consequently, each face of T is subdivided into four triangles in T''. Clearly, the resulting triangulation T'' triangulates the same surface S. (See Figure 6.)

Any 3-colouring of the medial graph T' can be regarded as a very particular four-colouring of T'', in which every original vertex $i \in V$ (of degree d_i) is coloured 4, and the vertices in V' (of degree six in T'') are coloured $1, 2, 3$ in such a way the resulting four-colouring is proper. The Kempe changes on T' can be viewed as a subset of the full set of possible Kempe changes we can perform on T'': In particular, we can only

choose the induced subgraphs T''_{ab} with $a, b \in \{1, 2, 3\}$.

We can regard the edge-colourings of a triangulation T as constrained colourings on T''; and we can use all the technology we have for standard four-colourings of triangulations (in particular, the notion of the colouring degree) [20].

These observations hold for every triangulation T. In this paper, we are focusing on the triangulations $T = T(3L, 3M)$ of the torus. For these particular triangulations, the corresponding medial graphs $T' = M(T) = T'(3L, 3M)$ are kagomé graphs embedded on a torus. It is easy to see that the graph T'' is isomorphic to the triangulation $T(6L, 6M)$ in this case. (See Figures 3 and 7 for an explicit example with $L = M = 1$.)

(a)   (b)
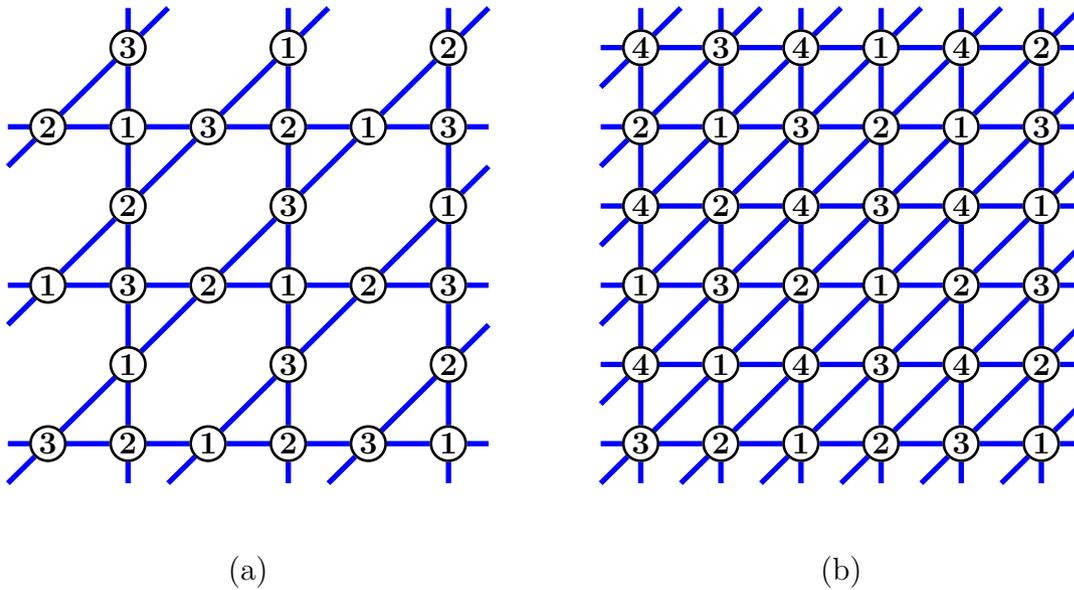
Figure 7. Different colourings of the triangulation $T(3,3)$ and their interpretation. (a) The representation of the edge-colouring g given in Figure 3(b) as a three-colouring h of the medial graph $T'(3,3)$, which is a kagomé graph embedded on a torus. (b) The representation of the three-colouring h on $T'(3,3)$ as a four-colouring of $T''(3,3) = T(6,6)$. [Notice that this panel is obtained from Figure 3(b) by periodically shifting the later one step to the left, and by placing a spin coloured 4 on every intersection of the edges in Figure 3(b).]

Given the triangulation $T = T(3L, 3M)$, the set of proper four-colourings on $T'' = T(6L, 6M)$ is denoted $\mathcal{C}_4(T'')$; the set of constrained proper four-colourings of T with all vertices in V coloured 4 and those in V' coloured $1, 2, 3$, will be denoted $\widetilde{\mathcal{C}}_4(T'')$. The colourings in $\widetilde{\mathcal{C}}_4(T'')$ will be referred to as the *special four-colourings* of T''.

Let us summarize the described correspondence in the following proposition:

Proposition 3.3 *Let us consider a triangulation T embedded on a surface S. Then, there is a bijective correspondence between the three–edge-colourings of T and the three-colourings of the vertices of its medial graph $T' = M(T)$. Furthermore, if $T = T(3L, 3M)$, then T' is a subgraph of $T'' = T(6L, 6M)$ and there is a bijection*

between the three-colourings of the vertices of the medial graph $T' = M(T)$ and the special four-colourings of T''. Under these two correspondences, K-equivalence is preserved.

The main lemma we need is the following:

Lemma 3.4 *Let us consider the set of edge-colourings of the triangulation $T(3L, 3M)$. If the set of special four-colourings of $T(6L, 6M)$ contains an element f with $\deg(f) \equiv 6$ (mod 12), then there are at least two Kempe equivalence classes for edge-colourings of $T(3L, 3M)$. In other words, there are at least two Kempe equivalence classes for the vertex three-colourings of the medial graph $T'(3L, 3M)$.*

PROOF. First of all, let us prove that there is an element $h \in \widetilde{\mathcal{C}}_4(T(6L, 6M))$ with $\deg(h) = 0$. This colouring will belong to one Kempe equivalence class for edge-colourings of $T(3L, 3M)$. This four-colouring can be constructed as follows: We start with the standard three-colouring of $T'' = T(6L, 6M)$, which always exists as both dimensions are multiple of three. Next, we change the colour of every vertex in T'' coming from the original triangulation $T = T(3L, 3M)$ (viewed as a special vertex in T'') into the colour 4. Recolouring of each such vertex is a Kempe change on T'', so this gives a special colouring h that is K-equivalent to the three-colouring of T''. Since the degree of the three-colouring is 0 and changing the colour of a single vertex preserves the degree of the colouring, we conclude that $\deg(h) = 0$.

Suppose now that there is another proper four-colouring f of $T(6L, 6M)$ belonging to $\widetilde{\mathcal{C}}_4(T(6L, 6M))$ and such that $\deg(f) \equiv 6 \pmod{12}$. Theorem 3.5 of [20] ensures that the four-colourings h and f are not K-equivalent on the larger configuration space $\mathcal{C}_4(T(6L, 6M))$. Thus, this conclusion holds if we restrict to the smaller space $\widetilde{\mathcal{C}}_4(T(6L, 6M)) \subseteq \mathcal{C}_4(T(6L, 6M))$ of special four-colourings. ∎

Remark. The proper 3–colouring h described in the above proof for $T'(3L, 3L)$ corresponds to the so-called '$\sqrt{3} \times \sqrt{3}$' ordered state in the physics literature [8].

4. Main result

The goal of this section is to prove the following theorem:

Theorem 4.1 *Let $T = T(3L, 3L)$ be a triangulation of the torus with $L \in \mathbb{N}$. Then there are at least two Kempe equivalence classes of edge three-colourings of T. In other words, the WSK dynamics for the three-state Potts antiferromagnet at zero temperature on the kagomé graph $M(T) = T'(3L, 3L)$ with $L \in \mathbb{N}$ is not ergodic.*

PROOF. The basic strategy is similar to that of the proof of Theorem 3.5 of Ref. [20]: We will explicitly construct a four-colouring of $T''(3L, 3L) = T(6L, 6L)$ with the desired properties, and then, we apply Lemma 3.4. To avoid ambiguities in the computation of the degree, we orient $T(6L, 6L)$ and $\partial\Delta^3$ in such a way that the boundary of all

triangular faces are always followed clockwise. The contribution of a triangular face t of $T(6L, 6L)$ to the degree of a given colouring f is $+1$ (resp. -1) if the colouring is 123 (resp. 132) if we move clockwise around the boundary of t. In our figures, those faces with orientation preserved (resp. reversed) by f are depicted in light (resp. dark) gray. We split the proof in two cases, depending on the parity of L.

The simpler case is when L is odd, i.e., $3L = 6k - 3$ for an integer $k \geq 1$. We only need to prove that there exists a special four-colouring $f \in \widetilde{\mathcal{C}}_4(T)$ of the triangulation $T = T''(6k - 3, 6k - 3) = T(12k - 6, 12k - 6)$ with $\deg(f) \equiv 6 \pmod{12}$. This four-colouring is just the standard non-singular four-colouring c_{ns}. In particular, for a generic triangulation $T(3L, 3M)$, this non-singular four-colouring c_{ns} is given by:

$$c_{\mathrm{ns}}(x, y) = \begin{cases} 1 & \text{if } x, y \equiv 1 \bmod 2 \\ 4 & \text{if } x \equiv 1 \text{ and } y \equiv 0 \bmod 2 \\ 2 & \text{if } x \equiv 0 \text{ and } y \equiv 1 \bmod 2 \\ 3 & \text{if } x, y \equiv 0 \bmod 2 \end{cases}, \quad 1 \leq x \leq 3L, 1 \leq y \leq 3M. \tag{7}$$

Its existence for every triangulation $T(12k - 6, 12k - 6)$ with $k \in \mathbb{N}$ is given by Proposition 3.2 of Ref. [20]. In addition, c_{ns} for $T = T(12k - 6, 12k - 6)$ has all vertices of $V(6k - 3, 6k - 3)$ (and only these) coloured 4; therefore, it belongs to the restricted set $\widetilde{\mathcal{C}}_4(T)$. Finally, its degree is given by $\deg(c_{\mathrm{ns}}) = 2(6k-3)^2 \equiv 6 \pmod{12}$.

Remark. The proper 3–colouring on $T'(6k - 3, 6k - 3)$ associated to the special 4–coloring c_{ns} on $T(12k - 6, 12k - 6)$ corresponds to the so-called $Q = 0$ state in the physics literature [7].

CASE 2: $L = 2k$. The above proof does not work for the triangulations $T(6k, 6k)$, as the non-singular four-colouring of $T''(6k, 6k) = T(12k, 12k) := T$ has degree $\equiv 0 \pmod{12}$. We will describe the required four-colouring of T by a construction made in four steps. The idea is to build the target four-colouring by using counter-diagonals of the triangular lattice: these counter-diagonals are orthogonal to the inclined edges of the triangulation when embedded on a square grid, and will be denoted $\mathrm{D}j$, $j = 1, 2, \ldots, 12k$. In Figure 8 we show the triangulation $T(6, 6)$, along with its six counter-diagonals $\mathrm{D}j$. As we have embedded the triangulation into a square grid, we will use Cartesian coordinates (x, y), $1 \leq x, y \leq 3L$, for labelling the vertices.

Let us consider the triangulation $T = T(12k, 12k)$ with $k \in \mathbb{N}$. (We will illustrate the main steps with the case $k = 1$). Our construction consists of four steps:

Step 0. To simplify the notation, let us first colour 4 those vertices in the vertex set $V' = V(T(6k, 6k)) \subset V(T)$. In our standard representation of the triangulation T as a square grid with diagonal edges, we see that the vertex located at (x, y), $1 \leq x, y \leq 12k$, belongs to V' if and only if $x \equiv 1 \pmod{2}$ and $y \equiv 0 \pmod{2}$.

Step 1. On the counter-diagonal D1 we colour 2 the $6k$ vertices not already coloured 4. On D2, we colour 1 the vertices with x-coordinates either equal to $x = 1$ or $6k + 1 \leq x \leq 12k$. The other $6k - 1$ vertices on D2 are coloured 3. On $\mathrm{D}(12k)$,
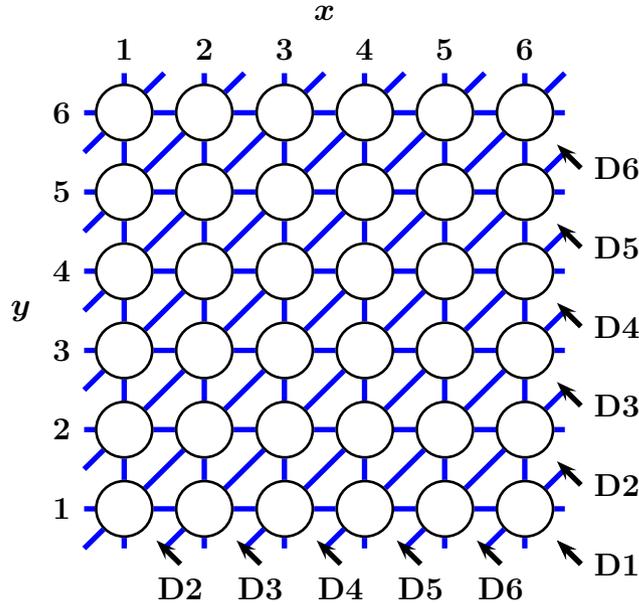
Figure 8. Notation used in the proof of Theorem 4.1. Given a triangulation $T(M, M)$ (here we depict the case $M = 6$), we label each vertex using Cartesian coordinates (x, y), $1 \leq x, y \leq M$. The arrows (pointing north-west) show the counter-diagonals Dj with $j = 1, \ldots, M$.

we colour all vertices 1 or 3 in such a way that the resulting colouring is proper (for each vertex there is a unique choice).

We colour all vertices on D3 and $D(12k - 1)$ using colour 2, except those vertices belonging to V'. Finally, we colour all vertices on D4 and $D(12k - 2)$ using colours 1 and 3 (again, for each vertex the choice is unique). The resulting colouring is depicted on Figure 9. Currently, the partial degree of f is $\deg f|_R = 6$, where we define the *partial degree* as the contribution of all triangles already coloured 123 (contribution $+1$) or 132 (contribution -1) towards the degree of the targeted colouring f.

Step 2. There are $12k - 7$ counter-diagonals to be coloured, and in this step we will sequentially colour all of them but five. (Observe that there is nothing to do if $k = 1$.) This will be done by performing the following procedure: Suppose that we have already coloured counter-diagonals Dj and $D(12k - j + 2)$ ($j \geq 4$) using colours 1 and 3. We first colour $D(j + 1)$ and $D(12k - j + 1)$ using colour 2 for all vertices not belonging to V'. We then colour $D(j + 2)$ and $D(12k - j)$ using colours 1 and 3. In these cases, for each vertex we have only one choice. This step is repeated $3(k - 1)$ times: We add $12(k - 1)$ counter-diagonals, and there are only five counter-diagonals not coloured yet. Indeed, the last coloured counter-diagonals use colours 1 and 3, as at the end of Step 1.

Each of these $3(k - 1)$ steps adds a 4 to the degree of the colouring. Namely, all new triangles coloured 123 or 132 are located along the counter-diagonals $D(j + 1)$ and $D(12k - j - 1)$. Triangles coloured 123 and 132 come in pairs, annihilating each other's contribution, except at the vertex coloured 2 where colour 3 is changed to 1 on the next counter-diagonal. There we get two triangles, each contributing $+1$, on each of the
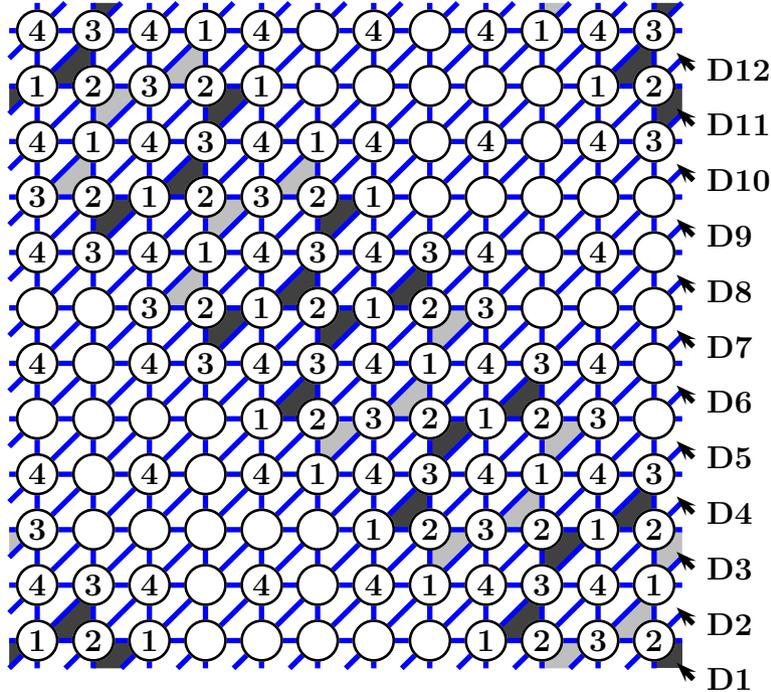
Figure 9. The four-colouring of $T(12, 12)$ after the first step of the algorithm given by the proof of Case 2 of Theorem 4.1. All vertices belonging to the set V' are already coloured 4.

counter-diagonals $D(j+1)$ and $D(12k-j-1)$. Thus, the partial degree of the colouring is $\deg f|_R = 6 + 12(k-1)$.

Step 3. The last coloured counter-diagonals are $D(6k-2)$ and $D(6k+4)$.

On $D(6k-1)$, there is a single vertex not in V' whose colour can only be 2 since it has neighbours of colours 1, 3, and 4. This vertex is located at $x = 9k - 1$ (resp. $x = 3k$) if k is odd (resp. even). We then colour the vertex $v_0 = (x_0, y_0)$ on $D(6k-1)$ located at $x_0 = 3k - 1$ (resp. $x_0 = 9k$) using colour 1 (resp. 3) if k is odd (resp. even). The remaining vertices on $D(6k-1)$ are coloured 2.

On $D(6k)$ we find that there are two vertices that are neighbours of v_0 and should be coloured 2. These vertices are located at $(x_0, y_0 + 1)$ and $(x_0 + 1, y_0)$ (valid for every k). The other vertices on $D(6k)$ are coloured 1 or 3; the choice is unique for each vertex. As shown in Figure 10, the contribution to the degree of these new triangular faces is 2; thus, the partial degree of f is $\deg f|_R = 8 + 12(k-1)$.

Step 4. On $D(6k+1)$ the vertices at (x_0+2, y_0) and (x_0, y_0+2) (where the special vertex $v_0 = (x_0, y_0)$ was defined in the previous step) should be coloured 1 and 3, respectively. The other vertices are coloured 1 or 3 (the choice among these two possible colours is again unique for each vertex).

On $D(6k + 3)$, we find that the vertex at $x = x_0 + 2$ should be coloured 2. The other vertices on this counter-diagonal and not belonging to V' are coloured 1 or 3; the choice among these two colours is again unique.
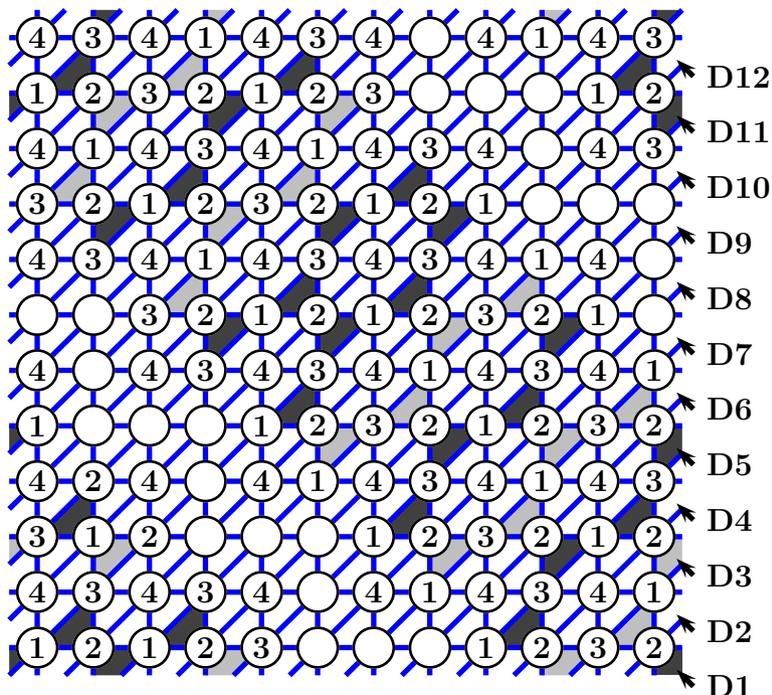
Figure 10. The four-colouring of $T(12, 12)$ after Step 3 of the algorithm given by the proof of Case 2 of Theorem 4.1
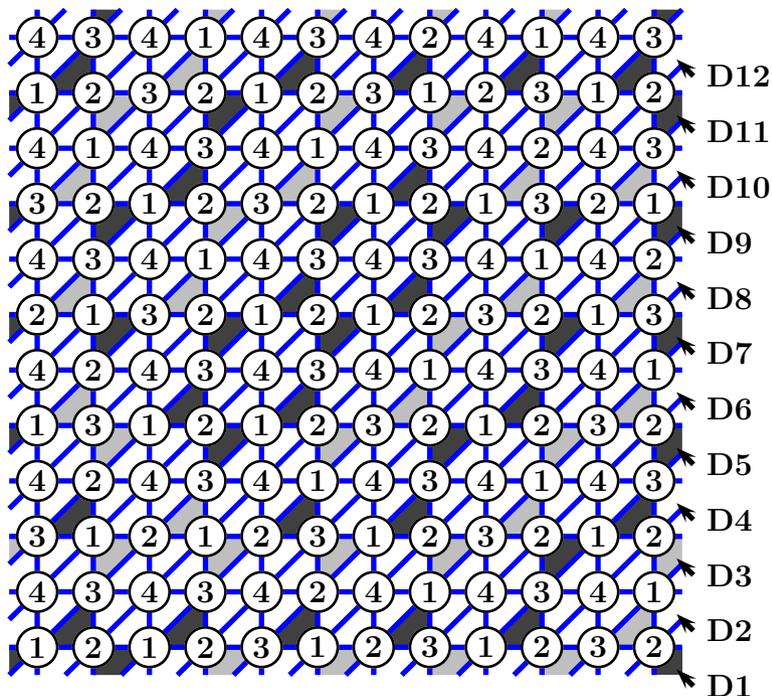
Figure 11. The four-colouring of $T(12, 12)$ after Step 4 of the algorithm given by the proof of Case 2 of Theorem 4.1

Finally, every vertex on D($6k + 2$) has its colour fixed by their neighbours. All of them are coloured 2 except two vertices: the vertex at $x = x_0 + 2$ is coloured 3, and the

vertex at $x = x_0 + 1$ is coloured 1. The sought colouring is depicted in Figure 11. In this case, the increment in the degree is -2. Therefore, the degree of the final four-colouring is

$$\deg f \;=\; 6 + 12(k-1) \;\equiv\; 6 \quad (\mathrm{mod}\ 12) \tag{8}$$

This colouring f of $T(12k, 12k)$ is proper, belongs to the restricted set $\widetilde{\mathcal{C}}_4(T(12k, 12k))$ and its degree is congruent to six modulo 12, as claimed. ∎

The following Corollary follows trivially:

Corollary 4.2 *The single-site dynamics for the three-state Potts antiferromagnet at zero temperature on the kagomé graph $T'(3L, 3L)$ with $L \in \mathbb{N}$ is not ergodic.*

PROOF. It follows from the fact that single-site moves are a subset of the Kempe moves. In fact, each proper 3–colouring of the kagomé graph $T'(3L, 3L)$ is an ergodicity class in the single-site dynamics. This is a consequence of each vertex belonging to two neighbouring triangular faces. Therefore, in every proper 3–colouring, every vertex has two neighboring vertices coloured with any of two possible other colours, and no change is possible. Therefore, each proper 3–colouring is *frozen* in the single-site dynamics, and constitutes an ergodicity class. ∎

References

[1] Potts R B, 1952 *Proc. Cambridge Philos. Soc.* **48** 106.
[2] Wu F Y, 1982 *Rev. Mod. Phys.* **54** 235; Erratum 1983 **55** 315.
[3] Wu F Y, 1984 *J. Appl. Phys.* **55** 2421.
[4] Salas J and Sokal A D, 1997 *J. Statist. Phys.* **86** 551 (arXiv:cond-mat/9603068).
[5] Aizenman M and Lieb E H, 1981 *J. Statist. Phys.* **24** 279.
[6] Chow Y and Wu F Y, 1987 *Phys. Rev.* B **36** 285.
[7] Chalker J T, Holdsworth P C W and Shender E F, 1992 *Phys. Rev. Lett.* **68** 855.

[8] Huse D A and Rutenberg A D, 1992 *Phys. Rev.* B **45** 7536.

[9] Chandra P, Coleman P and Ritchey I, 1993 *J Physique I* **3**, 591.

[10] Henley C L, 2009 *Phys. Rev.* B **80** 180401 (arXiv:0811l.0026).

[11] Bremaud P, 1999 *Markov Chains, Gibbs Fields, Monte Carlo Simulation and Queues*. Texts in Applied Mathematics. (Springer-Verlag, Berlin-Heidelberg).

[12] Landau D P and Binder K, 2009 *A Guide to Monte Carlo Simulations in Statistical Physics*, 3rd edition. (Cambridge University Press, Cambridge).

[13] Wang J–S, Swendsen R H and Kotecký R, 1989 *Phys. Rev. Lett.* **63** 109.

[14] Wang J–S, Swendsen R H and Kotecký R, 1990 *Phys. Rev.* B **42** 2465.

[15] Gibbons A, 1985 *Algorithmic graph theory*. (Cambridge University Press, Cambridge).

[16] Hutchinson J and Wagon S, 1998 *Am. Math. Monthly* **105** 170.

[17] Mohar B, *Kempe equivalence of colorings* 2006 *Graph Theory in Paris, Proc. Conf. in Memory of Claude Berge*, ed J A Bondy, J Fonlupt, J L Fouquet, J C Fournier and J J Ramírez Alfonsín (Birkhauser, Basel), pp. 287–297.

[18] Privman V, *Finite–Size Scaling Theory* 1990 *Finite Size Scaling and Numerical Simulations of Statistical Systems*, ed V Privman (World Scientific, Singapore), pp. 4–98

[19] Kano K and Naya S, 1953 *Prog. Theor. Phys.* **10** 158.

[20] Mohar B and Salas J, 2009 *J. Phys. A: Math. Gen.* **42** 225204 (arXiv:0901.1010).

[21] Fisk S, 1973 *Adv. Math.* **11** 326.

[22] Fisk S, 1977 *Adv. Math.* **24** 298.

[23] Fisk S, 1977 *Adv. Math.* **25** 226.

[24] Kasteleyn P W and Fortuin C M, 1969 *J. Phys. Soc. Japan* **26** (Suppl.) 11.

[25] Fortuin C M and Kasteleyn P W, 1972 *Physica* **57** 536.

[26] Sokal A D, *The multivariate Tutte polynomial (alias Potts model) for graphs and matroids* 2005 *Surveys in Combinatorics, 2005*, ed B E Webb (Cambridge University Press, Cambridge–New York), pp. 173–226 (arXiv:math.CO/0503607).

[27] Altschulter A 1971 *Discrete Math.* **1** 211.

[28] Burton J K and Henley C L, 1997 *J. Phys. A: Math. Gen.* **30** 8385 (arXiv:cond-mat/9708171).

[29] Ferreira S J and Sokal A D, 1999 *J. Stat. Phys.* **96**,461 (arXiv:cond-mat/9811345).

[30] Lubin M and Sokal A D, 1993 *Phys. Rev. Lett.* **71** 1889.

[31] M. Jerrum, private communication.